

STUDY OF ELASTIC AND INELASTIC SCATTERING OF DEUTERONS BY ${}^9\text{Be}$ AT ENERGY $E = 14.5$ MeV*

M. NASSURLLA^{a,b}, N. BURTEBAYEV^{a,b}, D.M. JANSEITOV^{a,c,b}
ZH. KERIMKULOV^a, D. ALIMOV^{a,b}, A.K. MORZABAYEV^d
K. TALPAKOVA^{a,d}, Y. MUKHAMEJANOV^a, L.I. GALANINA^e
A.S. DEMYANOVA^f, A.N. DANILOV^f, V. STARASTSIN^f

^aInstitute of Nuclear Physics, Ibragimova 1, 050032 Almaty, Kazakhstan

^bal-Farabi Kazakh National University, al-Farabi 71, 050040 Almaty, Kazakhstan

^cJoint Institute for Nuclear Research, Joliot-Curie 6, 141980 Dubna, Russia

^dL.N. Gumilev Eurasian National University

Satpayev 2, 010008 Nur-Sultan, Kazakhstan

^eSINP Moscow State University, Leninskie gory 1(2), 119991 Moscow, Russia

^fNRC Kurchatov Institute, Akademika Kurchatova pl. 1, 123182 Moscow, Russia

(Received December 11, 2019)

Differential cross sections have been measured for the elastic and inelastic scattering of deuterons on ${}^9\text{Be}$ at $E_d = 14.5$ MeV. As a result, we obtained new experimental data for the $d+{}^9\text{Be}$ elastic and inelastic scattering leading to the 2.43 MeV ($5/2^-$) excited state of the ${}^9\text{Be}$ nucleus. The experimental results on elastic scattering were analyzed within the framework of the optical model using the Woods–Saxon and double folding potentials. The theoretical calculations for the relevant excited states were performed using the coupled channel (CC) method. The optimal deformation parameters for the excited states of the ${}^9\text{Be}$ nucleus were extracted.

DOI:10.5506/APhysPolB.51.751

1. Introduction

A standard tool to study nuclear structure is the scattering of light projectiles, like protons, deuterons or ${}^3,{}^4\text{He}$, by a target nucleus, the structure of which is going to be studied. This method is based on the angular distribution measurements of the projectile-like products with fixed excitation energy in the (in)elastic and transfer reaction channels.

* Presented at the XXXVI Mazurian Lakes Conference on Physics, Piaski, Poland, September 1–7, 2019.

It has been shown that in light nuclei the nucleons tend to group into clusters, relative motion of which defines to a large extent the properties of these nuclei. The ${}^9\text{Be}$ nucleus is a unique example of a stable nuclear system presenting a cluster structure. The excited nucleus ${}^9\text{Be}^*$ can decay either directly into the $\alpha + n + \alpha$ three-body system or through one of the unstable nuclei, such as ${}^5\text{He}$ or ${}^8\text{Be}$. Relatively recent experimental studies [1, 2] explicitly confirm the cluster structure of ${}^9\text{Be}$. In addition to the cluster structure, in Ref. [3], it was suggested that the first excited state in ${}^9\text{Be}$ at 1.68 MeV ($1/2^+$) has an increased radius similar to nuclei with neutron halo.

Several papers have reported investigations on elastic and inelastic scattering of protons [4], deuterons [5–7], ${}^3\text{He}$ [8, 9] and α particles [10–12] on ${}^9\text{Be}$. For example, the interaction of deuterons [6, 7] and α particles [12] with ${}^9\text{Be}$ nuclei was analyzed using distorted wave Born approximation (DWBA) and coupled-channel (CC) models with phenomenological potentials. Later, certain excited states of ${}^9\text{Be}$ were analyzed in the framework of the CC method using phenomenological and folding potentials [8, 9]. Considering that ${}^9\text{Be}$ is a well-studied nucleus, it is surprising at first glance that new information on states fed in β -decay is found at energy as low as 5 MeV [13].

In this work, differential cross sections of elastic and inelastic deuteron scattering on ${}^9\text{Be}$ were measured at $E(d) = 14.5$ MeV, and we attempted to find the optimal deformation parameters for the ${}^9\text{Be}$ nucleus from a theoretical description of the experimental data on inelastic scattering leading to the excited state at 2.43 MeV ($5/2^-$) within the coupled channels method. This paper is a part of our extensive study of the cluster structure of the ${}^9\text{Be}$ nucleus.

2. Results and discussion

The experiment was performed using ${}^2\text{H}$ ion beams at 14.5 MeV energy delivered by the accelerator facilities at the Institute of Nuclear Physics (Almaty, Kazakhstan). The target was a self-supporting thin beryllium foil (99%) with a thickness of about $330 \mu\text{g}/\text{cm}^2$. The ΔE - E method was used for detection and identification of reaction products. The telescope detectors consisted of ΔE surface-barrier silicon detectors from ORTEC, $50 \mu\text{m}$ thick, followed by complete absorption E detectors of 1 mm thickness, used as stop detectors. A more detailed description of the experimental set-up is given in Ref. [14]. An energy spectrum for the $d+{}^9\text{Be}$ reaction at 50° angle is shown in Fig. 1 (a).

Calculations of differential cross sections of elastic scattering of deuterons on ${}^9\text{Be}$ were performed within the framework of the optical model (OM) with the Woods–Saxon (WS) and double folding (DF) potentials using the FRESKO code [15]. Our total real potential for these cases consists of the

nuclear (V_{nuc}), spin–orbit (V_{so}) and Coulomb (V_{C}) potentials

$$U(r) = V_{\text{nuc}}(r) + V_{\text{so}}(r) (\bar{l}s) + V_{\text{C}}(r). \quad (1)$$

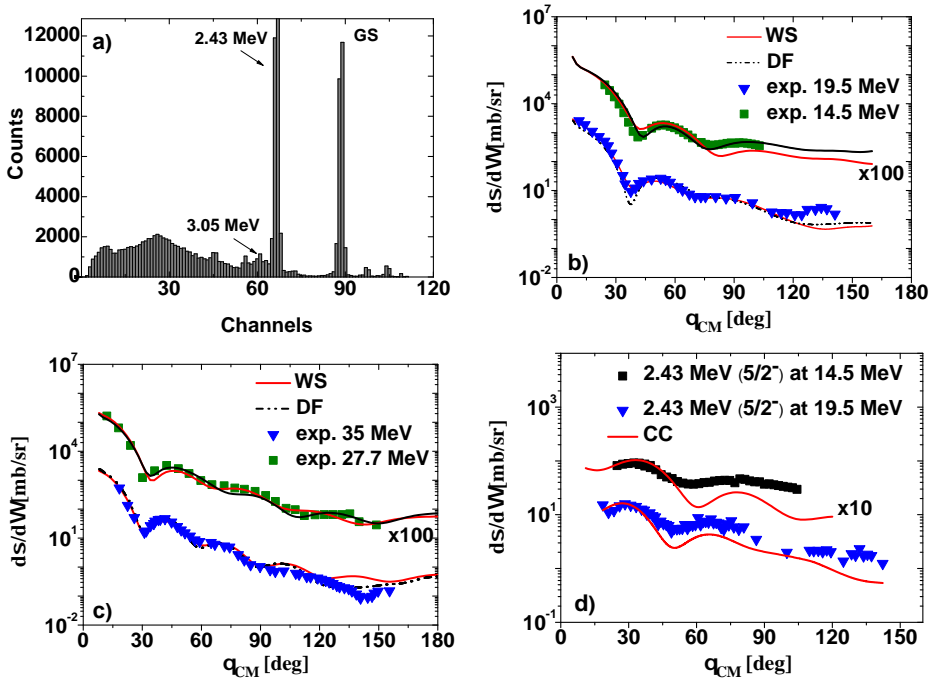


Fig. 1. (a) A typical energy spectrum for ${}^9\text{Be}(d, d){}^9\text{Be}$ at 50° angle; (b) and (c) Comparison between the experimental data and the calculated differential cross section for elastic scattering of deuterons from ${}^9\text{Be}$ at 14.5 MeV, 19.5 MeV [5], 27.7 MeV [6] and 35 MeV [5] energies, using the Woods–Saxon (WS) and double folding (DF) potentials; (d) Comparison between the experimental data and the calculated differential cross section for inelastic scattering of deuterons from ${}^9\text{Be}$ (2.43 MeV, $(5/2^-)$) at energies of 14.5 and 19.5 MeV within the CC framework.

The microscopic nuclear potential that we have also used to analyze the experimental data for the $d+{}^9\text{Be}$ system was based on the DF model [16]. DF potential is calculated by using the nuclear matter distributions of both projectile and target nuclei together with an effective nucleon–nucleon interaction potential (ν_{NN}). Thus, the DF potential is given as

$$V^{\text{DF}}(R) = \int d\mathbf{r}_1 \int d\mathbf{r}_2 \rho_p(\mathbf{r}_1) \rho_t(\mathbf{r}_2) \nu_{NN}(\mathbf{r}_{12}), \quad (2)$$

where $\rho_p(\mathbf{r}_1)$ and $\rho_t(\mathbf{r}_2)$ are the nuclear matter density distributions of the projectile and target nuclei, respectively. Gaussian density distributions (GD) were used for the both nuclei [17].

The effective nucleon–nucleon interaction, ν_{NN} , is integrated over both density distributions. Several expressions for the nucleon–nucleon interaction can be used for the folding model potentials. We have chosen the most common one, the M3Y (Michigan-3-Yukawa) realistic nucleon–nucleon interaction. The M3Y has two forms, one corresponds to M3Y-Reid [18] and another is based on the so-called M3Y-Paris interaction [19].

The real part of the optical model was obtained by using the above-described DF model, and we adopted the WS form for the imaginary potential.

Therefore, for the nucleon–nucleon-DF potential case, the nuclear potential consists of a real and an imaginary part

$$U^{\text{DF}}(r) = N_r V_{\text{DF}}(r) + iW(r), \quad (3)$$

where N_r is the normalization factor, which is determined from the fit of the OM calculation to the experimental data.

The comparison between the experimental data and the theoretical predictions for ${}^9\text{Be}(d, d){}^9\text{Be}$ at 14.5 MeV, 19.5 MeV [5], 27.7 MeV [6] and 35 MeV [5] energies is shown in Fig. 1 (b) and (c). The calculations use the potential parameters listed in Table I. The experimental data and theoretical calculations in Fig. 1 (b), (c) and (d) are multiplied by a factor of 100 and 10, respectively, in order to visually separate data at different energies. In Fig. 1 (b) and (c), the abbreviation WS corresponds to the calculations of the optical model with Woods–Saxon potential. DF corresponds to the calculations of the optical model with folding potential for the real part and imaginary potential taken from WS.

TABLE I

Potential parameters obtained for elastic scattering of deuterons from ${}^9\text{Be}$ at specific energies.

E [MeV]	Set	V [MeV]	r_V [fm]	a_V [fm]	N_r	W [MeV]	r_W [fm]	a_W [fm]
14.5	WS	95.14	1.17	0.88	1.5	16.03	1.32	0.64
	DF					16.03	1.32	0.64
19.0	WS	85.14	1.17	0.88	1.12	18.03	1.32	0.64
	DF					18.03	1.32	0.64
27.7	WS	80.14	1.17	0.7	1.16	24.03	1.32	0.48
	DF					24.03	1.32	0.48
35	WS	73.14	1.17	0.88	1.01	28.03	1.32	0.45
	DF					28.03	1.32	0.45

The global potential of Perey [20] is taken as the starting potential, but in our case, we changed some of its parameters. The standard phenomenological spin-orbit potential (along the spin of the target) allowed to improve the description of data at large angles using the following parameters: $V_{\text{so}} = 5.7$ MeV, $r_{\text{so}} = 1.07$ fm and $a_{\text{so}} = 0.66$ fm. To reduce the discrete ambiguity in determining the OP, the radii of the nuclear density distribution for the real (r_V) and imaginary (r_W) parts were fixed. The four remaining parameters of OP (V , W) and diffusions (a_V and a_W) were fitted to experimental data by χ^2 minimization.

In the OM calculations, the Coulomb radius $r_C = 1.3$ fm was adopted.

In the DF calculations, the normalization coefficient (N_r) for the real part of the potential was obtained to be between 1.01 and 1.5. The calculated elastic scattering cross sections are in good agreement with the available experimental data [5, 6] which are shown in Fig. 1 (b) and (c).

The angular distributions for the ($5/2^-$) excited state at 2.43 MeV in the ${}^9\text{Be}$ nucleus were analyzed within the coupled channel method. In the calculations, we used the WS potential. The comparison between the experimental data and theoretical predictions for the state at 2.43 MeV ($5/2^-$) at energies $E(d) = 14.5$ MeV and 19.5 MeV [5] are shown in Fig. 1 (d). For the calculations using the CC method, a significant discrepancy between the calculated cross sections for the excited state and the experimental data at low energies is observed. To improve their agreement, it is necessary to take into account the contribution of both the composite core and the strong coupled-channel effects, including the contributions of other excited states as, for example, in Ref. [8]. Calculations of differential cross sections for inelastic scattering were performed within the framework of the CC method using the ECIS88 code [21].

As mentioned above, in coupled-channel calculations we should provide parameters with information about the state in question, such as spin, parity and excitation energy. In addition, the deformation parameter is used as an adjustable parameter of calculation. As noted in Refs. [5, 22], the deformation parameter for the ${}^9\text{Be}$ nucleus is in the range of 0.65–0.8.

3. Summary

New experimental data have been obtained for the elastic and inelastic scattering of deuterons at the energy of 14.5 MeV from a ${}^9\text{Be}$ target, leading to the 2.43 MeV ($5/2^-$) excited state in ${}^9\text{Be}$. The data on elastic scattering were analyzed using two approaches, namely the phenomenological Woods–Saxon and semi-microscopic double folding potentials. For this analysis, we combined our new experimental results with literature elastic scattering data.

The data for the excited state were analyzed within the framework of the coupled-channel method at different energies.

The obtained deformation parameters for the ${}^9\text{Be}$ nucleus at 14.5 MeV are close to the values reported in Refs. [5, 22].

In the future, we plan to analyze the experimental data for transfer reactions induced by the $d+{}^9\text{Be}$ system, with exit channels such as $t+{}^8\text{Be}$, using the present optical potential parameters.

REFERENCES

- [1] T.A. Brown *et al.*, *Phys. Rev. C* **76**, 054605 (2007).
- [2] P. Papka *et al.*, *Phys. Rev. C* **75**, 045803 (2007).
- [3] A.S. Demyanova *et al.*, *JETP Lett.* **102**, 413 (2015).
- [4] N. Keeley *et al.*, *Phys. Rev. C* **99**, 014615 (2019).
- [5] B. Urazbekov *et al.*, *J. Phys. G: Nucl. Part. Phys.* **46**, 105110 (2019).
- [6] R.J. Slobodrian, *Nucl. Phys.* **32**, 684 (1962).
- [7] S. Tanaka *et al.*, *Jour. Phys. Soc. Jpn.* **45**, 733 (1978).
- [8] A.T. Rudchik *et al.*, *Nucl. Phys. A* **609**, 147 (1996).
- [9] D.M. Jansetov *et al.*, *Int. J. Modern Phys. E* **27**, 1850089 (2018).
- [10] R.B. Taylor, N.R. Fletcher, R.H. Davis, *Nucl. Phys.* **65**, 318 (1965).
- [11] S. Roy *et al.*, *Phys. Rev. C* **52**, 1524 (1995).
- [12] S.M. Lukyanov *et al.*, *J. Phys. G: Nucl. Part. Phys.* **41**, 035102 (2014).
- [13] Y. Prezado *et al.*, *Phys. Lett. B* **618**, 43 (2005).
- [14] Sh. Hamada *et al.*, *Phys. Rev. C* **87**, 024311 (2013).
- [15] I.J. Thompson, *Comput. Phys. Rep.* **7**, 167 (1988).
- [16] I.I. Gontchar, M.V. Chushnyakova, *Comput. Phys. Commun.* **181**, 168 (2010).
- [17] M. Karakoc, I. Boztosun, *Phys. Rev. C* **73**, 047601 (2006).
- [18] G. Bertsch *et al.*, *Nucl. Phys. A* **284**, 399 (1977).
- [19] N. Anantaraman, H. Toki, G.F. Bertsch, *Nucl. Phys. A* **398**, 269 (1983).
- [20] C.M. Perey, F.G. Perey, *Phys. Rev.* **132**, 755 (1963).
- [21] J. Raynal, computer codes ECIS-88, NEA-0850.
- [22] A. Szczurek *et al.*, *Z. Phys. A* **333**, 271 (1989).